Int. Nano Lett., Vol. 1, No. 2, July 2011, pp. 103-110.

Computational Study of Hydrogen Adsorption on Potassium-Decorated Boron Nitride Nanotubes

Md. Shahzad Khan, Mohd. Shahid Khan*

Department of Physics, Jamia Millia Islamia, Central University, New Delhi, India

(Received 22 January 2011, Accepted 3 March 2011)

We have investigated the potassium-decorated boron nitride nanotubes for hydrogen storage using semi-empirical AM1 method. The ultra narrow (3,3) and (5,0) boron nitride nanotubes of same diameter but of different chirality have been used. Both of them show hydrogen storage greater than 8% by weight. Density of States have been calculated and it is found that the presence of alpha density of state of potassium results in smaller energy gap as a result of which the conductivity of the potassium decorated boron nitride nanotubes is enhanced compared to pristine boron nitride nanotubes. Charge decomposition analysis showed that there is significant transfer of charge from adsorbate potassium to boron nitride nanotubes; the same is also confirmed by Mulliken Population analysis. For the same diameter, due to different electronic configurations, zigzag tube is found to be slightly more favourable for hydrogen adsorption. The results of the present simulation study suggest that the potassium decorated boron nitride nanotubes are good candidates for hydrogen adsorption.

Keywords: Potassium decorated, Boron nitride nanotubes, Semi empirical method, Hydrogen storage, Binding energy, Density of states

Introduction

Safe and efficient hydrogen adsorption requirement for future fuel cell vehicle (FCV) has raised the demand for simulation study of adsorption of hydrogen on nanostructures. Recently several studies have been carried out on Carbon based materials such as nanotubes [1-6], fullerenes [7,8], metal hydride and metal–organic-frame works [9,10]. The binding energy of adsorption of hydrogen on the pristine single-wall carbon nanotube (SWCNT) is very small [5]. However, it has been reported that the carbon nanomaterials, when coated with alkali and alkaline earth atoms, can be used for hydrogen storage [11-13]. In contrast to SWCNTs which are semiconductor or metallic, depending on their diameter and helicities, the boron nitride nanotubes (BNNTs) that have features similar to carbon nanotubes are wide band gap semiconductor with their band gap just independent of tube diameter and helicity [14]. Also, Boron nitride nanotubes are more stable both thermally and chemically [15-17]. These unique properties of BNNTs open a path for interesting research in order to examine these as potential candidates for hydrogen adsorption. It has been reported by *Ma et al* [18] that the multiwalled and bamboo like BNNTs can absorb hydrogen up to 2.6 wt % at room temperature wherein 70% of the hydrogen is chemisorbed. *Tang et al.* [19] found that hydrogen storage even reach up to 4.2 wt% if the BNNTs were treated with Platinum. These theoretical studies suggested that metal-doped BNNTs hold some potential as hydrogen storage media. The Pt-doped [20], Ti-doped [21], and Si-doped [22] BNNTs have been examined, and the results of these studies proved that the capacity for hydrogen storage in the doped BNNTs is enhanced as a result of doping (or decorating) as compared to pristine BNNTs and BN clusters. These studies

---

[*] Corresponding Author:
E-mail: *mskhan@jmi.ac.in*
Tel: +91 112 698 4631, Fax: +91 112 698 1753

have also highlighted the importance of the surface area of BNNTs in hydrogen uptake of the nanostructures [23].

Keeping these findings in mind we have selected relatively light alkali earth metal as a candidate for decoration on hydrogen terminated BNNTs. Hydrogen-termination has been used to avoid the boundary effect. Being a light metal, potassium gives little weight contribution to effective storage material, however adsorbing good amount of hydrogen molecules leads to the increase of hydrogen storage by wt. The aim of the present work is to examine the extent up to which the K-decorated BNNTs enhance the hydrogen uptake using the semi empirical AM1 method [24], which has been used widely to calculate various properties at small computational cost for wide variety of materials [25-32].

Model system and computational method

The geometry optimizations of all the structures leading to energy minima were carried using the AM1 self-consistent fields molecular orbital (SCFMO) method at the unrestricted Hartree Fock (UHF) level. The structures were initially optimized using the MM+ molecular mechanics method and then were optimized using AM1 method employing the steepest-descent optimizer followed by conjugate gradient, Fletcher–Reeves and Polak-Ribiere methods consecutively with convergence limit of 0.0001 kcal/mol and RMS gradient limit of 0.001 kcal/A-mol. All the calculations were performed using the HyperChem (7.1) package program [33]. For the charge decomposition analysis and PDOS, the single point calculations were carried out, the results of which were then used as input for the AOMIX [34, 35] program.

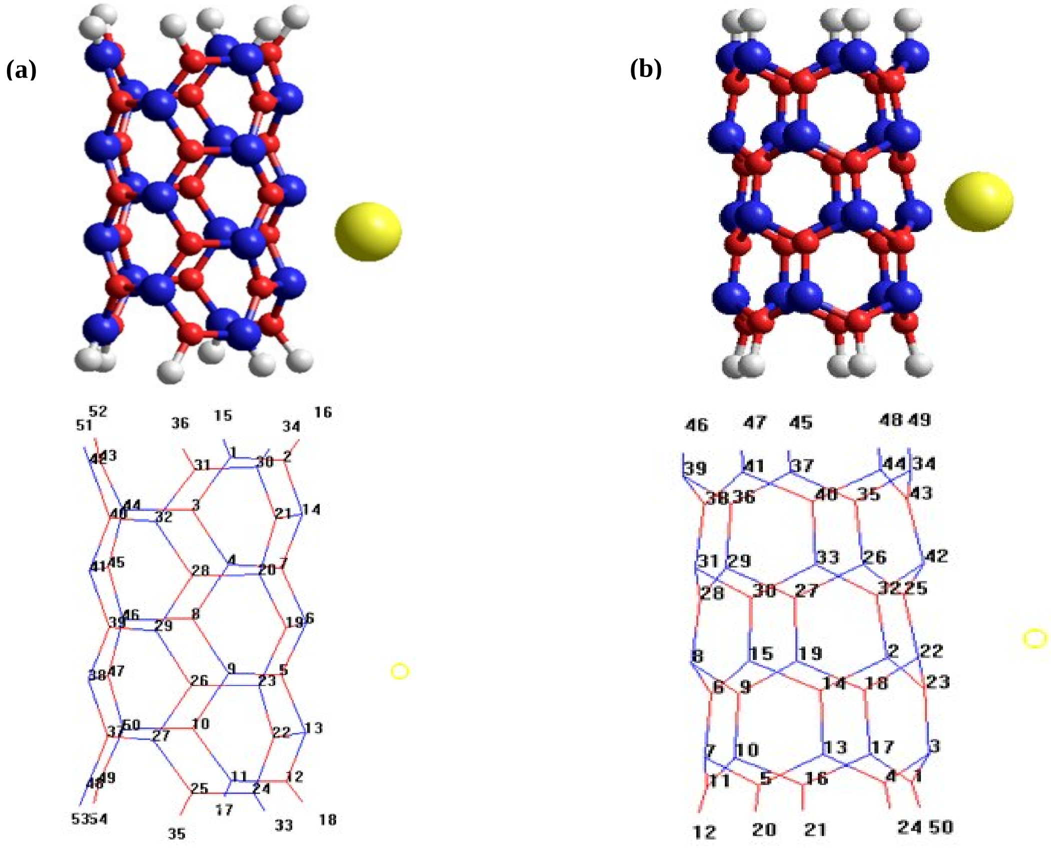
(a)
(b)
52 51 36 15 34 16
43 31 1 30 2
40 44 32 3 21 14
41 45 28 4 20 7
39 46 29 8 19 6
38 47 26 9 23 5
37 50 27 10 22 13
48 49 25 11 24 12
53 54 17 35 33 18
46 47 45 48 49
39 41 37 44 34
38 36 40 35 43
31 29 33 26 42
28 30 27 32 25
8 15 19 2 22
6 9 14 18 23
7 10 13 17 3
11 5 16 4 1
12 20 21 24 50

Fig. 1. AM1 Optimized structure of K(yellow)-decorated (a) (3,3) and (b) (5,0) BNNT(red ball for nitrogen and blue for boron atom).

Table 1. The changes of bond length of the associated mesh of BNNTs after doping and adsorption of Potassium.

3,3 BNNT			5,0 BN		
Bond length In (Å)	Pristine BNNT	K-Doped BNNT	Bond length In (Å)	Pristine BNNT	K-Doped BNNT
B5-B13	1.4653	1.5064	B25-N42	1.4655	1.5045
B5-N6	1.4601	1.4435	B25-N22	1.4437	1.4321
B19-N6	1.4596	1.5927	B23-N22	1.4675	1.5398
B19-N23	1.4523	1.5100	B23-N2	1.4675	1.5398
B22-N13	1.4432	1.4831	B32-N42	1.4655	1.5045
B22-N23	1.4690	1.4510	B32-N2	1.4675	1.4321

Results and discussion

Armchair (3,3) and zigzag (5,0) ultra-narrow boron nitride nanotubes (BNNTs) terminated with hydrogen atoms, each having 15 meshes, have been selected for the present study. Both of these have different chirality but are diametrically almost equal and both are wide band gap semiconductors. Fig. 1a,b show the AM1 optimized structures obtained after one K-atom was relaxed in the neighborhood of the already optimized structure of the pristine (3,3) and (5,0) BNNT respectively. As can be seen from these figures, AM1 force-field optimization resulted in the adsorption of the K-atom on the surface of the exterior wall of the optimized structures of (3,3) and (5,0) BNNTs. The AM1 optimized bond lengths in the mesh near the dopant K-atom before and after doping potassium atom on the (3,3) and (5,0) BNNTs are listed in Table 1, from which a distortion of BNNTs after potassium doping can be observed. The same is also apparent in Fig. 1a,b from which it can be seen that the K-atom occupies the hollow site on one of the hexagon of the BNNT. Adsorption energy of K atom doped on BNNT is evaluated according to the expression:

$$E_{ads} = E\,(NT+K) - E\,(NT) - E\,(K) \qquad (1)$$

where E (NT+K) is energy of K-doped BNNT, E (NT) is energy of nanotube and E (K) is free energy of potassium atom.

The process of adsorbing K-atom on BNNTs is found to be exothermic with binding energy of 3.2 eV/K-atom and 2.8 eV/K-atom for (3,3) and (5,0) BNNT respectively. *Margine et al* [36] reported that the presence of strong electron donor alkali metals on BNNTs provided positive potential surrounding alkali atoms. The same phenomenon has been observed here for K-doped BNNTs having dipole moment of 9.5 D and 9.7 D respectively for (3,3) and (5,0) K-doped BNNT, with the dipole originating from centre of tube and passing through decorated potassium atom. And it is well supported by Mulliken charge analysis which revealed a charge transfer of 0.697e from decorated potassium atom to (3,3) BNNT and 0.71e to (5,0) BNNT respectively. The redistribution of charge within BNNT is markedly over the mesh which is nearest to potassium atom. The boron constituent still has positive charge which has been slightly reduced, while negative charge on nitrogen has increased a little. The main contributions to the HOMO and LUMO in K-doped BNNTs are from nearest neighboring atoms of potassium and have feeble participation of s and p-orbital from potassium side. On the other hand for pristine BNNTs, the HOMO is largely consisted of p orbital of constituent nitrogen atoms and LUMO consists of s-orbital of boron atoms. In order to examine the effect of K-doping on the electronic structure of BNNTs, the PDOS of the doped BNNTs are plotted and are shown in Fig. 2. It is the presence of potassium atom due to which the contribution to inter-frontier orbitals by the labeled constituents got manifested. The electronic state of the alpha DOS of decorated sample changes. The conductivity of BNNTs gets enhanced due to appearance of a peak on the top of valence band in the presence of potassium adsorbate.

Adsorption of a single H_2

The H_2 molecule can be adsorbed to the K-decorated BNNTs through K-atom with distance of 2.5Å and 2.49Å from K-atom in (3,3) and (5,0) K-decorated BNNTs respectively. The two H-K bond lengths are 2.52 Å and 2.54 Å for both the (3,3) and (5,0) BNNTs, however, there is slight elongation in H-H bond length in (5,0)BNNTs. Binding-energy value is 0.53 eV/ H_2 molecule for K-doped (3,3) BNNT while in case of (5,0) nanotube it is slightly less, 0.51eV/ H_2 molecule. The predicted adsorption energy is defined as:

$$E_{ads} = E\ (K+BNNT + n\ H_2) - E\ [K+BNNT -(n-1)\ H_2] - E\ (H_2) \qquad (2)$$

where n is the number of free hydrogen molecule.

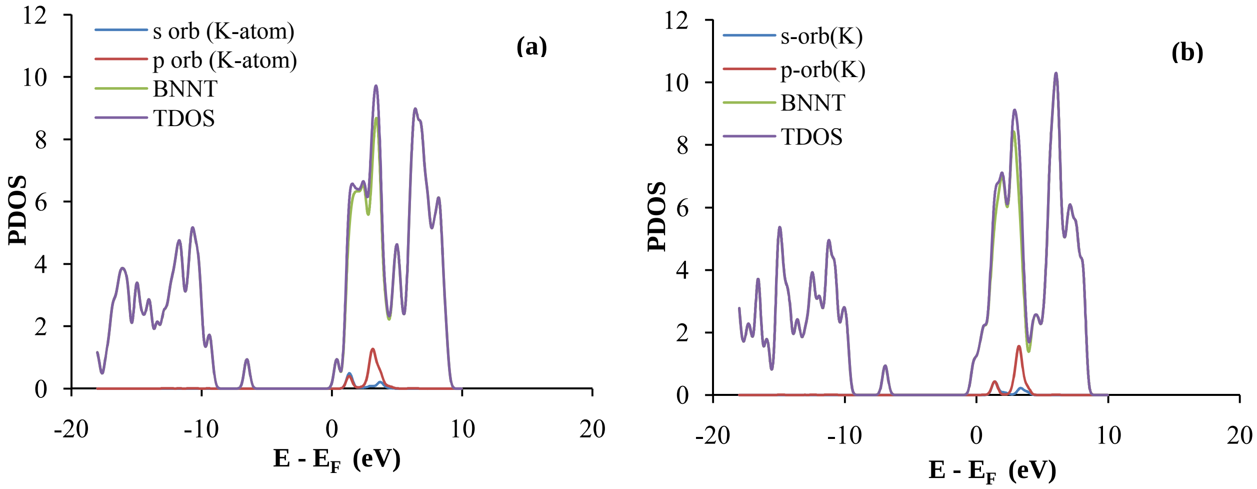

Fig. 2. (a) PDOS for K-Doped (3,3) BNNT and (b) K-doped (5,0) BNNT is plotted. Colour online represents the various fragments.

As can be seen in Fig. 3 the orientation of hydrogen molecule is side-on with respect to K-atom in both the nanotubes. Fig 4 shows the PDOS of the single H_2 molecule adsorbed on the (3,3) and (5,0) K-decorated BNNTs. The PDOS analysis by considering H_2 molecule, potassium atom and BNNT as individual fragments, revealed that it is the hybridization of the empty K-4p orbitals with H_2 σ orbital that contribute to the H_2 adsorption for both (3,3) and (5,0) nanotubes. The charge decomposition analysis (CDA) considering K-atom and a single H_2 molecule as fragment-1 and (3,3) BNNT as fragment-2 revealed that there is a net charge donation of 0.847 electrons for alpha MOs from fragment-1 to fragment-2. In case of alpha DOS, for beta DOS there is a charge donation of 0.156 electrons from fragment-2 to fragment-1. Similarly, for K-doped (5,0) BNNT, a net charge donation of 0.853 electrons from fragment-1 to fragment-2 takes place for alpha DOS whereas a net charge donation of 0.148 electrons is predicted from fragmen-2 to fragment-1 in case of beta MOs. These donations are net result of donation from fragment-1 to fragment-2 and back-donation from fragment-2 to fragment-1. The self-polarization of fragment orbital plays almost negligible role in charge transfer. The Mullikan population analysis (MPA) revealed that the hydrogen molecule has unequal charges (viz .050e and .029e) on its two atomic centres and it is slightly polar in nature as a result of which it seeks K-atom which carry 0.612e charge over it. It is suggested that the charge transfer leaves the metal dopant in cationic form so that the hydrogen molecule can be attracted by the metal cation via the charge polarization mechanism.

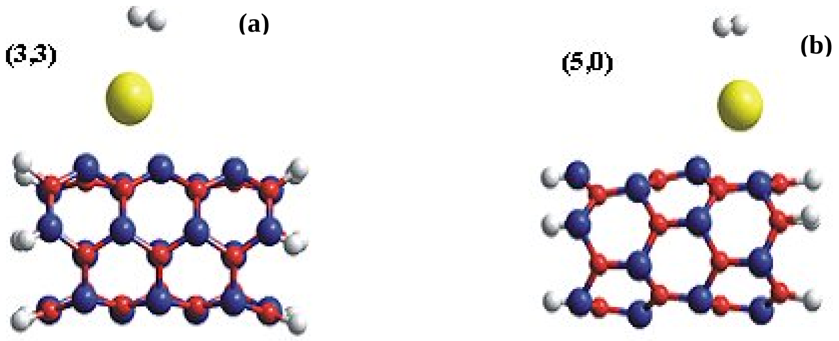

Fig. 3. H_2 molecule adsorbed on potassium decorated (3,3) and (5,0) BNNT.

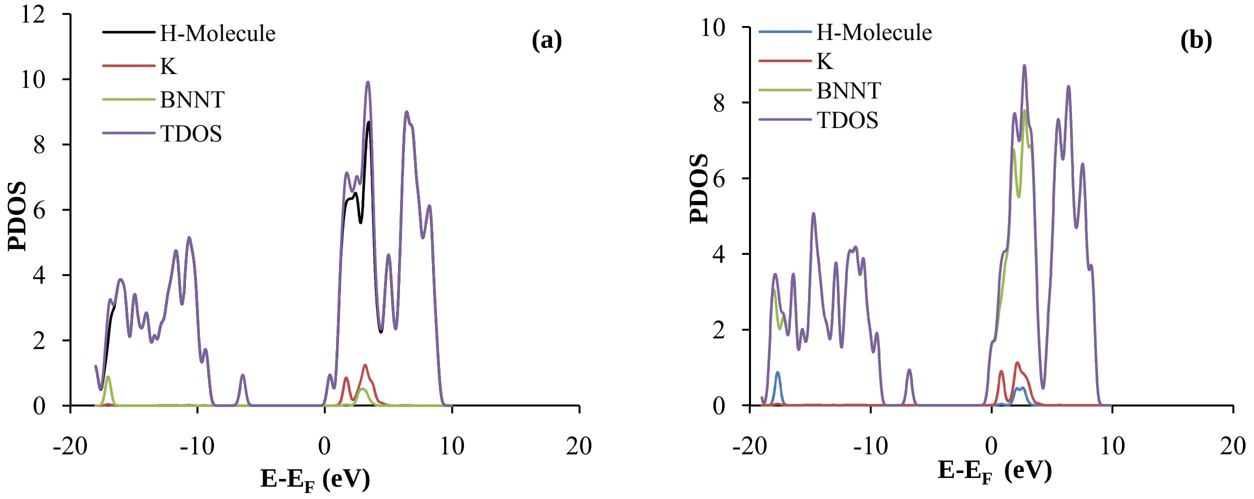

Fig. 4. PDOS for single H_2+ K-decorated BNNT (colour online are fragment wise selection), (a) for (3,3) and (b) for (5,0).

Adsorption of multiple H_2

The adsorption of 2nd H_2 molecule resulted in a decrease in binding energy per H_2 molecule for both (3,3) and (5,0) K-doped BNNT with values being 0.49 eV and 0.51eV per H_2 respectively. There is almost no change in bond length of H_2 molecules. Mulliken population analysis has shown that it is only the redistribution of charges between K-atom and H_2 molecules which is responsible for binding of the second H_2 molecule. The charge configuration on surface of BNNTs is affected negligibly by adsorption of 2nd hydrogen molecules. The K-atom is found to have a slightly reduced charge of 0.544e. On the other hand, the hydrogen molecules are observed to have unequal distribution of charge within their hydrogen atoms with values of 0.058e and 0.018e for the first H_2 and 0.059e and 0.014e on the 2nd H_2. On progressively adding more hydrogen molecules, the charge on K atom decreases. The charge on K-atom is found to be 0.339e for the adsorption of eight H_2 molecules. The optimization calculations for different number of H_2 molecules, for adsorption on K-doped BNNTs, were carried out. The calculated values of binding energy per hydrogen are presented in Table 2. It is found that one K atom can at most adsorb eight H_2 molecules with E_b of 0.38eV/ H_2 and 0.41eV/ H_2 for (3,3) and (5,0) BNNT respectively. Multiple hydrogen molecules adsorbed on K-doped BNNTs are shown in Fig. 5. These results indicate that the binding energy of H_2 has little to do with the chirality of BNNTs.

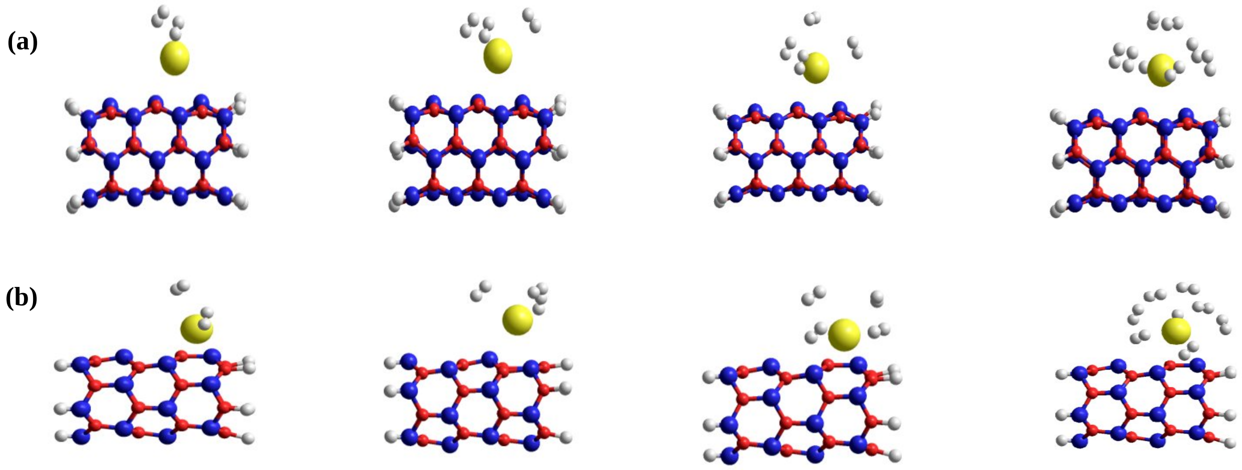

Fig. 5. Multiple Hydrogen adsorption on (a) K-Decorated (3,3) BNNT and (b) (5,0) BNNT.

Table 2. Binding energy per hydrogen molecule (in eV) on potassium decorated BN nanotube.

	$1H_2$	$2H_2$	$3H_2$	$4H_2$	$5H_2$	$6H_2$	$7H_2$	$8H_2$
3, 3 K-doped BNNT	0.51	0.49	0.48	0.45	0.43	0.41	0.40	0.38
5, 0 K-doped BNNT	0.53	0.51	0.50	0.48	0.46	0.44	0.42	0.41

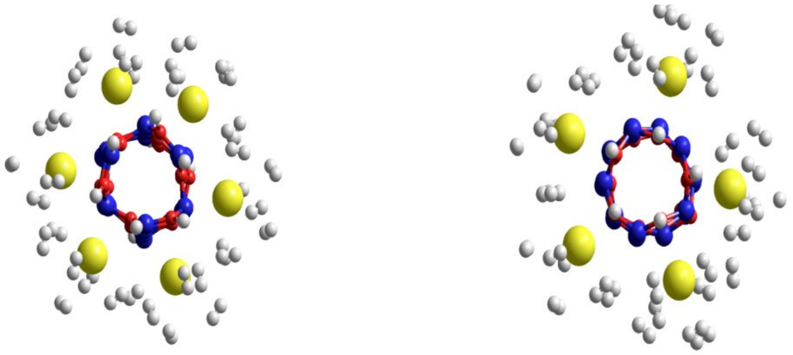

8.5% by wt of Hydrogen on (3,3) BNNT   9.4% by wt of Hydrogen on (5,0) BNNT

Fig. 6. 2/5 coverage of K-atom on (3,3) nanotube with 36 H_2 molecules adsorbed and 1/3 coverage on (5,0) with 37 H_2.

Hydrogen adsorption on high coverage K decorated BNNT

A further study for the stable K adsorbates with high coverage on boron nitride nanotube resulted in maximum coverage of 2/5 on the (3,3) and 1/3 on (5,0) nanotube with E_b being 2.3 eV and 2.8 eV, respectively. For (5,0) BNNT, a maximum coverage of 1/3 with K atoms can be made as clustering of K-atoms started with addition of more potassium atoms due to the nearest neighboring effect, as for the stable K adsorbates on boron nitride nanotube, K-K distances should be larger than that of bulk K. Similarly, maximum K converge of 2/5 is possible on (3,3) BNNT with 6-K atoms. The (3,3) K-decorated BNNT with maximum coverage of 2/5 is found to adsorb at most 36 H_2 with E_b of 0.41eV/ H_2, corresponding to a hydrogen uptake of 8.5% by wt . For (5,0) K-doped BNNT with maximum coverage, the number of H_2 molecules adsorbed is found to be 37 with E_b of 0.55eV/ H_2 with uptake of 9.4% by wt. The optimized molecular structures of these K-decorated BNNTs with maximum coverage and possible adsorbed hydrogen molecules are shown in Fig. 6. It can be inferred from these results that the zigzag (5,0) K-decorated BNNTs are more favourable for hydrogen adsorption.

Conclusion

The optimizations based on semi empirical AM1 method have been carried out for exploring the adsorption of the hydrogen on K-decorated BNNTs with chirality (3,3) and (5,0). It is found from the calculated PDOS for K-decorated BNNTs that due to the change in electron density of state of pristine nanotube, the conductivity of these K-decorated BNNTs is increased as a result of decoration with K-atoms. Charge decomposition analysis has indicated transfer of a significant amount of charge to nanotube from adsorbed K atom and H_2 molecule. It is the hybridization of empty K-4p orbital with H_2 σ orbital that leads to hydrogen adsorption. The binding energy of the K-atom is found to be independent of the chirality of the BNNTs. The coverage of K over nanotubes should not be much large as it causes clustering over nanotube. The maximum coverage of K atoms on (3,3) and (5,0) BNNTs resulted in 8.5% and 9.4% hydrogen storage by wt on BNNTs, respectively. The results of the present simulation study suggest that the K-decorated BNNTs are good candidates for hydrogen adsorption.

Acknowledgment

One of the authors, MSK, acknowledges the grant of financial support from Department of Science and Technology, New Delhi under the International Travel Support Scheme for attending and presenting this work in the XIX IMRC at Cancun, Mexico, during August15-19, 2010.

Reference

[1] A.C. Dillon, K.M. Jones, T.A. Bekkendahl, C.H. Kiang, D.S. Bethune, M.J. Heben, Nature 386 (1997) 377.
[2] S.P. Chan, G. Chen, X.G. Gong, Z.F. Liu, Phys. Rev. Lett. 87 (2001) 205502.
[3] O. Gulseren, T. Yildirim, S. Ciraci, Phys. Rev. Lett. 87 (2001) 116802.
[4] W.Q. Deng, X. Xu, W.A. Goddard, Phys. Rev. Lett. 92 (2004) 166103.
[5] S. Dag, Y. Ozturk, S. Ciraci, T. Yildirim, Phys. Rev. B: Condens. Matter 72 (2005) 155404.
[6] T. Yildirim, S. Ciraci, Phys. Rev. Lett. 94 (2005) 175501.
[7] Y. Zhao, Y.H. Kim, A.C. Dillon, M.J. Heben, S.B. Zhang, Phys. Rev. Lett. 94 (2005) 155504.
[8] T. Yildirim, J. Iniguez, S. Ciraci, Phys. Rev. B: Condens. Matter 72 (2005) 153403.
[9] B. Bogdanovic, M. Felderhoff, S. Kaskel, A. Pommerin, K. Schlichte, F. Schuth, Adv. Mater. 15 (2003) 1012.
[10] T. Yildirim, M. R. Hartman, Phys. Rev. Lett. 95 (2005) 215504.
[11] M. Yoon, S. Yang, C. Hicke, E. Wang, D. Geohegan, Z. Zhang, Phys. Rev. Lett. 100 (2008) 206806.
[12] H. Lee, J. Ihm, M. L. Cohen, S.G. Louie. Phys. Rev. B: Condens. Matter 80 (2009) 115412.
[13] W. Liu, Y.H. Zhao, Y.Li, Q. Jiang, E.J. Lavernia. J. Phys. Chem. C 113 (2009) 2028.
[14] X. Blase, A. Rubio, S.G. Louie, M.L. Cohen, Europhys. Lett. 28 (1994) 335.
[15] A. Loiseau, F. Willaime, N. Demoncy, G. Hug, H. Pascard, Phys. Rev. Lett. 76 (1996) 4737.
[16] E. Bengu, L.D. Marks, Phys. Rev. Lett. 86 (2001) 2385.
[17] V. Nirmala, P. Kolandaivel, J. Mol. Struct. THEOCHEM 817 (2007) 137.
[18] R. Ma, Y. Bando, H. Zhu, T. Sato, C. Xu, D.H. Wu, J. Am. Chem. Soc. 124 (2002) 7672.
[19] C. Tang, Y. Bando, X.X. Ding, S. Qi, D. Golberg, J. Am. Chem. Soc. 124 (2002) 14550.
[20] X. Wu, J.L. Yang, X.C. Zeng, J. Chem. Phys. 125 (2006) 044704.
[21] E. Durgun, Y.R. Jang, S. Ciraci, Phys. Rev. B: Condens. Matter 76 (2007) 073413.
[22] S.A. Shevlin, Z.X. Guo, Phys. Rev. B: Condens. Matter 76 (2007) 024104.

[23] A.M. Seayad, D.M. Antonelli, Adv. Mater. 16 (2004) 765.

[24] M.J.S. Dewar, E.G. Zoebisch, E.F. Healy, J.J.P. Stewart. J. Am. Chem. Soc. 107 (1985) 3902.

[25] S. Erkoc, J. Mol. Struct. THEOCHEM 542 (2001) 89.

[26] L. Turker, J. Mol. Struct. THEOCHEM 577 (2002) 205.

[27] M.S. Khan, Z.H. Khan, Can. J. Anal. Sci. Spectros. 47 (2002) 146.

[28] M.S. Khan, Z.H. Khan, Spectrochim. Acta, Part A 59 (2003) 1409.

[29] L. Turker, S. Gumus, J. Mol. Struct. THEOCHEM 681 (2004) 21.

[30] M.S. Khan, Z. H. Khan, Spectrochim. Acta, Part A 61 (2005) 777.

[31] V.A. Margulis, E.E. Muryumin, O.B. Tomilin, in: T.N. Veziroglu, S.Yu. Zaginaichenko, D.V. Schur, B. Baranwski, A.P. Shpak, V.V. Skorokhod, A. Kale (Eds.), Hydrogen Materials Science and Chemistry of Carbon Nanomaterials, Springer, Dordrecht, Netherlands, 2007.

[32] R. Goel, W.A. Siddigi, B. Ahmed, M.S. Khan, V.M Chaubey, Desalination 263 (2010) 45.

[33] Hyperchem 7.1, Hypercube Inc., USA.

[34] S.I. Gorelsky, Program for Molecular Orbital Analysis, University of Ottawa, Ottawa, 2007.

[35] S.I Gorelsky, A.B.P Lever, J. Organomet. Chem. 635 (2001) 187.

[36] E.R. Margine, V.H. Crespi, Phys. Rev. Lett. 96 (2006) 1968.